Journal of
Plant Ecology

VOLUME 1, NUMBER 4,
PAGES 247–257

DECEMBER 2008

doi: 10.1093/jpe/rtn025

available online at
www.jpe.oxfordjournals.org

Estimation of aboveground biomass using *in situ* hyperspectral measurements in five major grassland ecosystems on the Tibetan Plateau

Miaogen Shen[1], Yanhong Tang[2], Julia Klein[3], Pengcheng Zhang[4], Song Gu[5], Ayako Shimono[2] and Jin Chen[1,]*

[1] *State Key Laboratory of Earth Surface Processes and Resource Ecology, Academy of Disaster Reduction and Emergency Management, Beijing Normal University, Beijing 100875, China*
[2] *National Institute for Environmental Studies, Tsukuba, Ibaraki 305-8569, Japan*
[3] *Colorado State University, Fort Collins, CO 80523, USA*
[4] *Terrestrial Ecology Lab, Graduate School of Life and Environment Science, University of Tsukuba, Tennodai 1-1-1, Tsukuba, Ibaraki 305-8577, Japan*
[5] *Northwest Plateau Institute of Biology, Chinese Academy of Science, Xining 810001, China*
*Corresponding author. State Key Laboratory of Earth Surface Processes and Resource Ecology, College of Resources Science and Technology, Beijing Normal University, Beijing 100875, China. Tel: +86-10-58802876; Fax: +86-10-58802876; E-mail: chenjin@ires.cn

Abstract

Aims

There are numerous grassland ecosystem types on the Tibetan Plateau. These include the alpine meadow and steppe and degraded alpine meadow and steppe. This study aimed at developing a method to estimate aboveground biomass (AGB) for these grasslands from hyperspectral data and to explore the feasibility of applying air/satellite-borne remote sensing techniques to AGB estimation at larger scales.

Methods

We carried out a field survey to collect hyperspectral reflectance and AGB for five major grassland ecosystems on the Tibetan Plateau and calculated seven narrow-band vegetation indices and the vegetation index based on universal pattern decomposition (VIUPD) from the spectra to estimate AGB. First, we investigated correlations between AGB and each of these vegetation indices to identify the best estimator of AGB for each ecosystem type. Next, we estimated AGB for the five pooled ecosystem types by developing models containing dummy variables. At last, we compared the predictions of simple regression models and the models containing dummy variables to seek an ecosystem type-independent model to improve prediction of AGB for these various grassland ecosystems from hyperspectral measurements.

Important findings

When we considered each ecosystem type separately, all eight vegetation indices provided good estimates of AGB, with the best predictor of AGB varying among different ecosystems. When AGB of all the five ecosystems was estimated together using a simple linear model, VIUPD showed the lowest prediction error among the eight vegetation indices. The regression models containing dummy variables predicted AGB with higher accuracy than the simple models, which could be attributed to the dummy variables accounting for the effects of ecosystem type on the relationship between AGB and vegetation index (VI). These results suggest that VIUPD is the best predictor of AGB among simple regression models. Moreover, both VIUPD and the soil-adjusted VI could provide accurate estimates of AGB with dummy variables integrated in regression models. Therefore, ground-based hyperspectral measurements are useful for estimating AGB, which indicates the potential of applying satellite/airborne remote sensing techniques to AGB estimation of these grasslands on the Tibetan Plateau.

Keywords: biomass estimation • dummy variable • hyperspectral remote sensing • Tibetan Plateau • regression analysis • vegetation index • VIUPD

Received: 13 October 2008 Revised: 13 October 2008 Accepted: 13 October 2008

INTRODUCTION

The Tibetan Plateau may play a significant role in influencing climate because of its vast area and height and thermal influences on atmospheric circulation (Chapin *et al.* 2008; Kutzbach *et al.* 1993; Manabe and Terpstra 1974). Grasslands are the most extensive vegetation type covering the Tibetan Plateau, which covers an area of >2.5 million km^2. An accurate estimation of aboveground biomass (AGB) of the vegetation across this large area is needed to understand how the vegetation on the Plateau might influence climate, through changes in surface albedo or carbon storage. However, AGB in these grasslands is highly heterogeneous across the Plateau. While studies have investigated AGB across the Tibetan Plateau using direct field measurements at local sites (e.g. Fan *et al.* 2008), empirical ecological models across the plateau (e.g. Luo *et al.* 2002) and remotely sensed data for local regions (e.g. Kumpula *et al.* 2004), no appropriate approach is currently available to accurately estimate the AGB of these heterogeneous grasslands at lager spatial scales.

Remote sensing technology provides an important approach for estimating AGB at large spatial scales. To apply this technique, it is critical to understand the relationship between the AGB and spectral features of reflectance from aboveground vegetation (Friedl *et al.* 1994; Schino *et al.* 2003). Many studies have demonstrated that, among various kinds of spectral features, narrow-band vegetation indices are sensitive to variations in AGB. Holzgang (2001) found that the simple ratio calculated from reflectance in 808 and 677 nm can be used to assess the aboveground phytomass of sub-alpine and alpine grasslands. Hansen and Schjoerring (2003) evaluated the relationships between green biomass and all two-band combinations in the normalized difference vegetation index (NDVI) and revealed a number of grouped wavebands (mainly in the red-edge spectral region, from 680 to 750 nm) with high correlation for biomass estimation. Mutanga and Skidmore (2004a) found that the vegetation indices calculated from wavelengths located in the red edge are good estimators of pasture biomass at high canopy density. In a study of a Mediterranean shrubland, NDVI calculated from reflectance at 900 and 679 nm was found to be sensitive to both biomass and phenology changes (Filella *et al.* 2004). These studies demonstrate that vegetation indices are useful for estimating AGB within a single vegetation type. However, no general model of estimating AGB has been tested against multiple alpine ecosystems on the Tibetan Plateau.

Since there are various types of alpine ecosystems on the Tibetan Plateau due to its large spatial extension and high heterogeneity in water availability and temperature as well as anthropological activities, a large number of ground-truth data are required for developing AGB estimation models by using ecosystem type-dependent models. Moreover, such ecosystem type-dependent models may have different formulas and parameters. These make the estimation of AGB complicated and laborious across large spatial scales and heterogeneous landscapes. Therefore, a general ecosystem type-independent model for AGB estimation is needed.

The *in situ* hyperspectral data are of higher quality compared with data from satellite-borne sensors since there is little atmospheric effect and the solar-view geometry is strictly controlled. Therefore, the relationships between AGB and spectral features based on ground measurements are more reliable. Such relationships are required for building Spectra-AGB models with inputs of satellite data, especially in vegetation index (VI) selection and model form selection. In this study, we examined the relationships between AGB and each of seven narrow-band vegetation indices and that between AGB and the vegetation index based on universal pattern decomposition (VIUPD, Zhang *et al.* 2007) calculated from *in situ* hyperspectral data in five typical grassland ecosystems on the Tibetan Plateau. Our objectives were (i) to identify the best VI based on hyperspectral data—such a VI is also possibly collected by satellite/airborne sensors, for estimating the AGB for each ecosystem type on the plateau grasslands and (ii) to build a multiple-ecosystem model for estimating AGB independently of ecosystem type by evaluating the predictions of the multiple-ecosystem models with and without dummy variables.

METHODS

Study sites

Five grassland types (Table 1) were identified for the measurements of AGB and spectral reflectance based on their extensive spatial distribution on the Tibetan Plateau (Fig. 1 and Table 1). The measurements were taken between 24 July and 10 August 2006, when the AGB approached the annual maximum and was relative stable for a short duration of time. These five grasslands represent major grassland ecosystems on the Tibetan Plateau. The sampled ecosystems cover the areas with annual precipitation from 201 to 440 mm and annual mean temperature from −5.6 to 3.3°C. In each type of grassland, we measured the AGB and spectral reflectance in 12–15 circles, each with a radius of 15 cm. The 12–15 circles were selected to span relatively low to relatively high AGB within the grassland type in order to encompass large data variation for the models. Detailed information is provided in Table 1.

Measurements of biomass and spectral reflectance

Hyperspectral measurements of sampling circles were carried out at five sites along the Tibetan highway (Fig. 1). We made all the measurements between 10:00 and 14:00 h (local time) in clear sunshine. Spectrum measurements were taken using a portable spectroradiometer (MS-720, EKO Instrument Co. Ltd, Tokyo, Japan) and a white panel. The spectroradiometer sampling wavelength range is 350–1050 nm and its spectral resolution is 10 nm. The sensor, with a field of view of 25°, was mounted on a tripod at a zenith position of 67 cm above the

Table 1: location (longitude, latitude and altitude), vegetation characteristics, soil type, AGB indicated by mean ± standard deviation, sampling number (*N*) and soil water content of study sites

Ecosystems	*Kobresia* meadow	*Stipa* steppe	Degraded steppe	*Achnatherum* grassland	Degraded meadow
Longitude (°E)	91.9148	92.5925	99.5525	98.2270	92.3757
Latitude (°N)	32.8401	34.3279	36.7029	36.4412	34.1068
Altitude (m)	5142	4571	3571	3244	4736
Dominant species	*Kobresia pygmaea*	*Stipa purpurea*	*Oxytropis melancalyx, Carex sp.*	*Achnatherum splendens*	*Leontopodium leontopodioides, K.pygmaea*
Soil type[a]	Alpine meadow–steppe soils	Alpine steppe soils	Subalpine meadow soils	Typic brown pedocals	Alpine steppe soils
AGB (gm^{-2})[b]	232 ± 85	65 ± 31	218 ± 78	140 ± 83	94 ± 43
N	13	12	15	15	13
Soil water content (%)[c]	9.5	3.3	21.3	19.7	6
Precipitation (mm)[d]	439.7 (Anduo)	262.2 (Wudaoliang)	362.8 (Tianjun)	200.6 (Dulan)	282.6 (Tuotuohe)
Temperature (°C)[d]	−2.73	−5.60	−1.50	3.31	−4.22
Area (10^4 hm^2)[e]	5387.7	3166.9		160.8	1620

[a] According to soil map of China, 1979, edited by Nanjing Institute of Soil Science, Chinese Academy of Science.
[b] The mean of AGB was obtained from 12 to 15 circles at each site.
[c] Soil water content was measured with a time domain reflectometry when the spectral reflectance measurement was done.
[d] Precipitation and temperature are 18-year (1982–99) averages of annual mean values, calculated from daily data recorded by meteorological station nearest to the investigated site. Those inside brackets are the places where stations located in.
[e] The total area of grassland on the Tibetan Plateau is 11229.6×10^4 hm^2, of which alpine meadow covers an area of 5387.7×10^4 hm^2. Here, we consider that alpine meadow includes *Kobresia* meadow and degraded meadow. Both *Stipa* steppe and degraded steppe are considered as alpine steppe, which covers an area of 3166.9×10^4 hm^2 on the plateau. The area of *Achnatherum* grassland is considered as the area of humoral grassland since *Achnatherum* grassland is the dominant species of this kind of grassland on the plateau. These data are available on the Web site—http://www.grassland.net.cn/data/d61.htm. The area of the degraded meadow is according to Lan (2004).

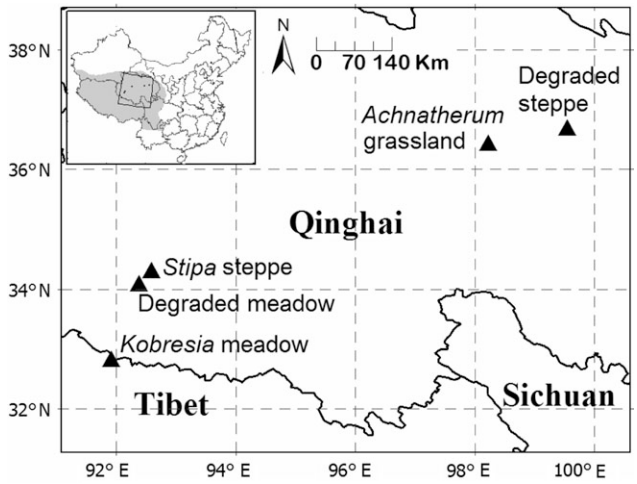

Figure 1: The Tibetan Plateau (gray) in China and locations of the investigated sites (solid triangles) on the plateau.

vegetation surface, which allowed coverage of a circular area with a radius of ~15 cm. The mean reflectance for each sampled circle was calculated as the average of five replicates. After the spectral measurement, the AGB of all the sampling circles was harvested. After oven drying for 48 h at 70°C, the resultant dry matter was weighed on an electronic scale with a sensitivity of 0.01 g. The spectra of the harvested pure vegetation and the soil surface after harvesting were both measured.

Data analysis

We calculated two categories of indices from the hyperspectral data: the narrow-band vegetation indices and the VIUPD. The narrow-band vegetation indices have been widely used and provide reliable estimates of canopy characteristics including leaf area index (LAI), chlorophyll concentration, nitrogen concentration, water content and biomass (Hansen and Schjoerring 2003; Kokaly and Clark 1999; Mirik *et al.* 2005; Mutanga and Skidmore 2004a, b; Thenkabail *et al.* 2000; Todd *et al.* 1998; Tucker 1977). VIUPD is a sensor-independent index that has been proved to be sensitive to vegetation signal (Zhang *et al.* 2007). Each of the vegetation indices and VIUPD were used as independent variables in linear regression models for estimating AGB for each of the five ecosystem types. We then built regression models between each of these independent variables and AGB for all the five ecosystems combined with dummy variables included to integrate effects of ecosystem type.

Narrow-band vegetation indices.

We used seven different narrow-band vegetation indices to evaluate their performance in AGB estimation. Because some of the study areas were sparsely vegetated, the enhanced vegetation index (EVI, Liu and Huete 1995), soil-adjusted vegetation index (SAVI, Huete 1988) and the modified soil-adjusted vegetation index (MSAVI, Qi *et al.* 1994) were used since they take soil background effects into consideration. We also

selected NDVI (Rouse *et al.* 1973), the chlorophyll-corrected triangular vegetation index (TVI, Hall and Rao 1987) and the simple ratio vegetation index (RVI, Jordan 1969) and difference vegetation index (DVI, Tucker 1979) as independent variables in estimating AGB (Table 2).

VIUPD.

VIUPD was developed from pattern decomposition and is sensitive to vegetation characteristics, especially under high LAI conditions (Zhang *et al.* 2007). VIUPD was developed from a linear spectral unmixing model with both vegetation and soil contained in the model; we used an identical approach in this analysis:

$$R_i(\lambda) = \mathrm{Cs}_i \mathrm{Ps}(\lambda) + \mathrm{Cv}_i \mathrm{Pv}(\lambda), \quad (1)$$

where $R_i(\lambda)$ was the measured reflectance of sample i, and $\mathrm{Ps}(\lambda)$ and $\mathrm{Pv}(\lambda)$ were normalized spectral patterns of pure soil and vegetation. $\mathrm{Ps}(\lambda)$ and $\mathrm{Pv}(\lambda)$ were calculated through normalization equations as

$$\mathrm{Ps}(\lambda) = \frac{R_s(\lambda)\int_{400}^{960} \mathrm{d}\lambda}{\int_{400}^{960} |R_s(\lambda)|\mathrm{d}\lambda}, \quad (2)$$

$$\mathrm{Pv}(\lambda) = \frac{R_v(\lambda)\int_{400}^{960} \mathrm{d}\lambda}{\int_{400}^{960} |R_v(\lambda)|\mathrm{d}\lambda}, \quad (3)$$

where $R_s(\lambda)$ and $R_v(\lambda)$ were the measured reflectance of pure soil and vegetation, respectively. Here, the wavelength range used was 400–960 nm to avoid water absorption of radiation around 980 nm. Cs_i and Cv_i were the decomposition coefficients. They could be obtained by ordinary least squares (OLS) method as same as the traditional unmixing method. After Cs_i and Cv_i were obtained, VIUPD was calculated as (revised from Zhang *et al*, 2007)

Table 2: narrow-band vegetation indices from reflectance used in estimating AGB of the alpine grasslands

VI	Equation	Reference
DVI	$\mathrm{DVI} = R_{875} - R_{680}$	Tucker (1979)
RVI	$\mathrm{RVI} = R_{875}/R_{680}$	Jordan (1969)
NDVI	$\mathrm{NDVI} = (R_{875} - R_{680})/(R_{875} + \mathrm{R}_{680})$	Rouse *et al.* (1973)
SAVI	$\mathrm{SAVI} = 1.5 \times (R_{875} - R_{680})/(R_{875} + R_{680} + 0.5)$	Huete (1988)
MSAVI	$\mathrm{MSAVI} = 0.5 \times [2 \times R_{875} + 1 - ((2 \times R_{875} + 1)^2 - 8 \times (R_{875} - R_{680}))^{0.5}]$	Qi *et al.* (1994)
TVI	$\mathrm{TVI} = 0.5 \times [120 \times (R_{750} - R_{550}) - 200 \times (R_{670} - R_{550})]$	Hall and Rao (1987)
EVI	$\mathrm{EVI} = 2.5 \times (R_{863} - R_{680})/(1 + R_{863} + 6 \times R_{680} - 7.5 \times R_{493})$	Liu and Huete (1995)

$$\mathrm{VIUPD} = \frac{\mathrm{Cv}_i - 0.1 \times \mathrm{Cs}_i}{\mathrm{Cs}_i + \mathrm{Cv}_i}. \quad (4)$$

Regression analysis.

Linear regression was used to develop regression model between AGB and each of the vegetation indices mentioned above. Because the relationship between AGB and VI might vary among different ecosystems, we analyzed the relationships for each of the five ecosystems separately. We then pooled the VI and AGB data for all five ecosystems and conducted the regression (referred to as the 'general model' below). We resized the sample for each site to 12 sample points by randomly dropping the excess data before building the general model since the different sample size in each site may exert extra impact on the dummy variables. To validate the general model, all 60 sample points (12 sample points for each ecosystem) of the five ecosystems were randomly separated into two data sets, one with 45 points for building model and the other with 15 points for testing the model. The model predictions were compared using root mean square error in prediction ($\mathrm{RMSE_P}$) calculated from the test data set.

$$\mathrm{RMSE_P} = \sqrt{\frac{\sum_{i=1}^{N} (\mathrm{AGB_{obs}} - \mathrm{AGB_{pre}})^2}{N}}, \quad (5)$$

where $\mathrm{AGB_{obs}}$ and $\mathrm{AGB_{pre}}$ were the observed and predicted AGB, respectively. N equals 15, the number of samples in the test data set.

The simple general regression model between each VI and AGB, where data from the five ecosystems were pooled, was specified as

$$\mathrm{AGB} = \beta_0 + \beta_1 \mathrm{VI} + \varepsilon. \quad (6)$$

In this model, the intercept and slope were obtained by OLS method (we refer to this as the 'simple general model' below).

Because the linear relationships between AGB and the vegetation indices maybe different for each ecosystem, we introduced dummy variables into the regression models to assess the impacts of ecosystem type. We compared these results with those of the simple linear regression model as specified by Equation (6).

Dummy variables are widely used to represent categorical variables in regression models. In this study, the dummy variables represented the five different ecosystem types. The regression model between AGB and VI containing dummy variables (referred to as the 'sophisticated general model' below) was

$$\begin{aligned}\mathrm{AGB} = {} & \beta_0 + \beta_1 \mathrm{VI} + \beta_2 D_1 + \beta_3 D_2 + \beta_4 D_3 + \beta_5 D_4 + \beta_6 D_1 \mathrm{VI} \\ & + \beta_7 D_2 \mathrm{VI} + \beta_8 D_3 \mathrm{VI} + \beta_9 D_4 \mathrm{VI} + \varepsilon,\end{aligned} \quad (7)$$

where VI was vegetation index such as NDVI, SAVI or VIUPD, D_1–D_4 were the dummy variables, β_0, β_1, …, β_9 were the regression coefficients and ε was random error. For example, if

Kobresia meadow was set as a bench ecosystem, the regression model between AGB and a VI could be specified using binary values assigned in Table 3. Here, the ecosystem for which D_1–D_4 were all assigned 0 was named as the bench ecosystem:

$$\textit{Kobresia}\ \text{meadow AGB} = \beta_0 + \beta_1 \text{VI} + \varepsilon,$$

$$\textit{Stipa}\ \text{steppe AGB} = \beta_0 + \beta_2 + (\beta_1 + \beta_6)\text{VI} + \varepsilon,$$

$$\text{Degraded steppe AGB} = \beta_0 + \beta_3 + (\beta_1 + \beta_7)\text{VI} + \varepsilon,$$

$$\textit{Achnatherum}\ \text{grassland AGB} = \beta_0 + \beta_4 + (\beta_1 + \beta_8)\text{VI} + \varepsilon,$$

$$\text{Degraded meadow AGB} = \beta_0 + \beta_6 + (\beta_1 + \beta_9)\text{VI} + \varepsilon. \quad (8)$$

We considered the differences in regression intercepts and slopes between VI and AGB in the regression functions for each ecosystem type. The difference between the intercepts and slopes was expected to be caused by the ecosystem type effects on the AGB–VI relationship since the vegetation type, canopy structure, phenological phase and soil type could vary among these ecosystems. In following sections, we use the form I(ecosystem type) and S(ecosystem type) to refer to the effects of a given ecosystem on the intercept and slope of the AGB–VI relationship, respectively. For example, β_2 and β_6 in Equation (8) indicate the effects of *Stipa* steppe on the intercept and slope of the AGB–VI relationship and they were written as I(*Stipa* steppe) and S(*Stipa* steppe), respectively.

To examine the ecosystem type dependence of dummy variable definition, the bench ecosystem was changed when implementing regression on AGB and VI. In detail, first *Kobresia* meadow was set as the bench ecosystem (Table 3) which was then replaced by *Stipa* steppe in another regression. Therefore, for each VI, five general regression models were obtained by setting each ecosystem as the bench ecosystem once, and their predictions were compared by RMSE_P calculated from the test data set.

The analysis provided tests of the significance for VI and ecosystem type effects on the regression and the significance of the model. Useful variables were selected by stepwise elimination of non-significant variables with large *P* values. In all the statistical tests in the study, we used $\alpha = 0.10$ as the cut-off for the null of hypothesis.

Table 3: an example of dummy variables values assignment in the general model for the five ecosystems in linear regression

D_1	D_2	D_3	D_4	If observation is for
0	0	0	0	*Kobresia* meadow
1	0	0	0	*Stipa* steppe
0	1	0	0	Degraded steppe
0	0	1	0	*Achnatherum* grassland
0	0	0	1	Degraded meadow

In this example *Kobresia* meadow was set as the bench ecosystem.

RESULTS

Spectral reflectance of the five ecosystems

A general vegetation spectral reflectance pattern was observed for all the five ecosystems on the Tibetan Plateau with higher reflectance in the near infrared (NIR) region due to mesophyll multiscattering and relatively low reflectance in the red region around a wavelength of 670 nm attributed to chlorophyll absorption (Fig. 2). The degraded steppe had the lowest reflectance ~0.06 in the red region due to strong absorption of chlorophyll since the study area was densely vegetated with a mean AGB of 218 gm^{-2}. Although *Kobresia* meadow had comparable AGB as the degraded steppe, the spectral curve of *Kobresia* meadow had higher reflectance in the red region and lower reflectance in the NIR region. For the other three sites, there was significantly higher reflectance in the red region and thus flatter uptrend from the visible to NIR region compared with either the degraded steppe or *Kobresia* meadow.

Relationships between AGB and VI in individual ecosystem

As shown in Table 4, when AGB of each ecosystem was estimated from the VI, all the regression models were significant (most *P* values < 0.01) with high coefficients of determination. The VI–AGB relationship with the highest R^2 for *Kobresia* meadow, *Stipa* steppe, the degraded steppe, *Achnatherum* grassland and the degraded meadow were RVI ($R^2 = 0.79$), RVI ($R^2 = 0.68$), VIUPD ($R^2 = 0.61$), SAVI ($R^2 = 0.86$), VIUPD ($R^2 = 0.71$) and RVI ($R^2 = 0.79$), respectively.

Though the coefficients of determination for the regression models were high, their values varied among different ecosystems. Among the five ecosystems, AGB of *Achnatherum* grassland and the degraded meadow, both of which were of middle vegetation density, was estimated with higher coefficients of determination than the other three ecosystems. In addition, for each of these two ecosystems, all eight vegetation indices estimated AGB with similar R^2 values. The R^2 values for *Kobresia* meadow were relatively higher than the densely vegetated degraded steppe and sparsely vegetated *Stipa* steppe. Additionally, for a given ecosystem with either high or low vegetation density, these various vegetation indices showed obviously different performance in estimating AGB.

Relationships between AGB and VI for five ecosystems

Simple regressions.

As shown in Table 5, each of the eight vegetation indices showed significant relationship with pooled AGB for all the five ecosystems (*P* value < 0.001). All the regressions had high

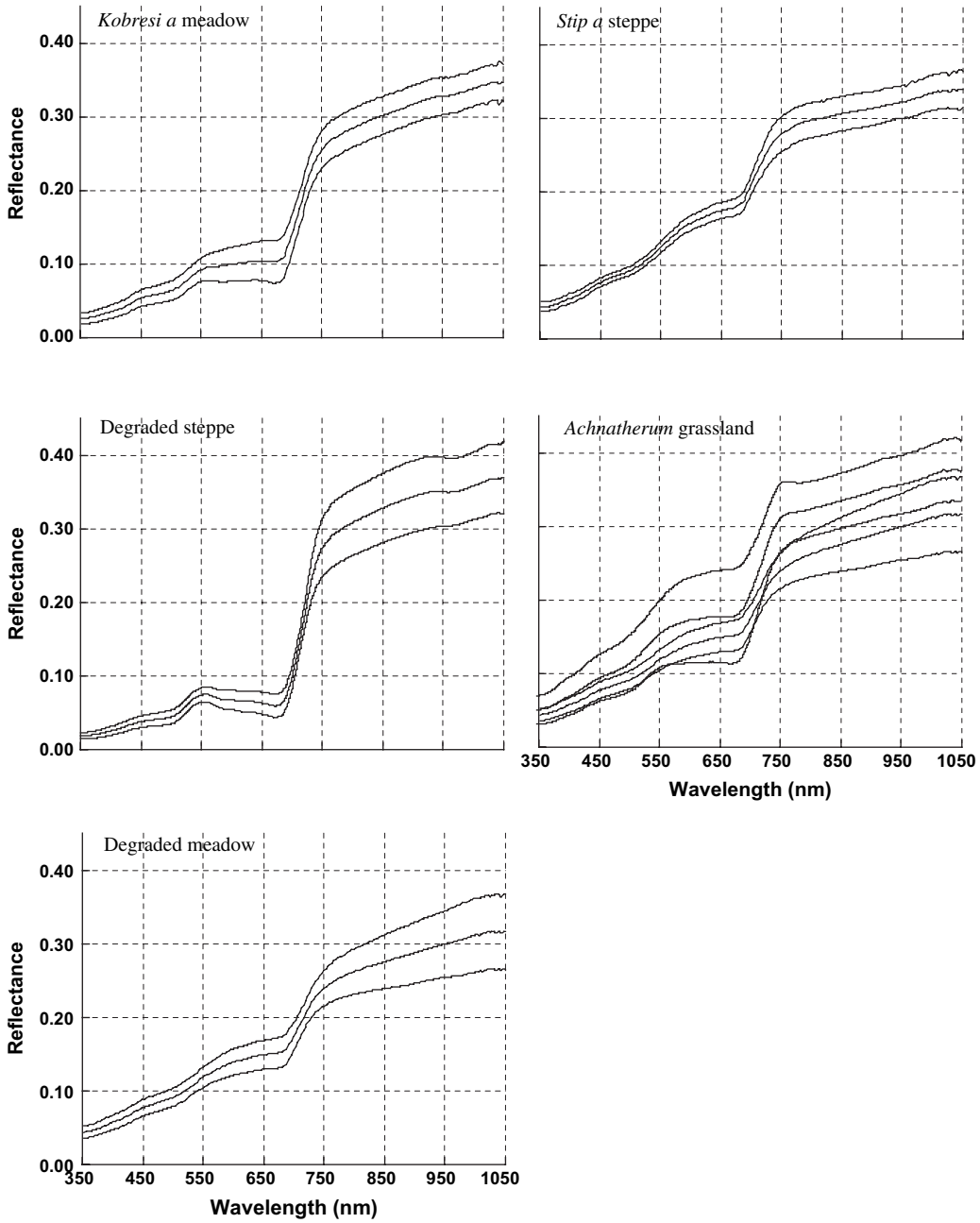

Figure 2: The spectral reflectance of different grasslands. The middle curve for each ecosystem indicates the mean reflectance from 12–15 circle areas with five replicates each. And the top and bottom lines for each ecosystem indicate the standard deviation of the spectral reflectance from the 12–15 circles.

coefficients of determination ($R^2 > 0.499$). The regression between AGB and VIUPD had the highest R^2 (0.734), followed by SAVI, NDVI, EVI, TVI, MSAVI, DVI and RVI. Accordingly, the regression model with higher R^2 values predicted AGB with higher accuracy, as indicated by $RMSE_P$ calculated from the 15 samples of the test data set. However, $RMSE_P$ values for most vegetation indices were $\sim$50 gm^{-2} which was a considerable fraction of 159.2 gm^{-2} as the mean of 15 samples of the observed AGB in the test data set.

Regression models containing dummy variables.

To seek a better estimate of AGB, dummy variables were added into regression models to integrate the effects of ecosystem type on the relationship between AGB and VI. Because VIUPD, SAVI and NDVI had the top three R^2 values in simple regression among all the eight vegetation indices (Table 5), each of these three vegetation indices and dummy variables corresponding to ecosystem types were used as independent variables to estimate AGB. Generally, the sophisticated general

Table 4: results of linear regression between AGB and various vegetation indices for each ecosystem separately

Ecosystems	*Kobresia* meadow	*Stipa* steppe	Degraded steppe	*Achnatherum* grassland	Degraded meadow
RVI (R^2)	0.79	0.68	0.58	0.82	0.79
P value	<0.001	<0.001	<0.001	<0.001	<0.001
DVI (R^2)	0.54	0.65	0.43	0.84	0.72
P value	0.003	0.002	0.008	<0.001	<0.001
NDVI (R^2)	0.73	0.67	0.57	0.86	0.78
P value	<0.001	0.001	0.001	<0.001	<0.001
SAVI (R^2)	0.65	0.67	0.49	0.86	0.76
P value	<0.001	0.001	0.004	<0.001	<0.001
MSAVI (R^2)	0.64	0.67	0.49	0.86	0.75
P value	<0.001	0.001	0.004	<0.001	<0.001
TVI (R^2)	0.56	0.54	0.45	0.84	0.78
P value	0.002	0.006	0.006	<0.001	<0.001
EVI (R^2)	0.64	0.67	0.46	0.85	0.76
P value	<0.001	0.001	0.005	<0.001	<0.001
VIUPD (R^2)	0.77	0.54	0.61	0.84	0.74
P value	<0.001	0.006	<0.001	<0.001	<0.001

Table 5: simple linear regression models between each VI and AGB for the five ecosystems using the data set for building model and the predictions of each model using an independent test data set

	Simple linear regression model (n = 45)		
VI	*P* value	R^2	$RMSE_P$ (n = 15)
DVI	<0.001	0.663	52.76
EVI	<0.001	0.673	52.17
MSAVI	<0.001	0.666	52.6
NDVI	<0.001	0.68	50.69
RVI	<0.001	0.499	60.45
SAVI	<0.001	0.685	50.93
TVI	<0.001	0.672	53.06
VIUPD	<0.001	0.734	49.81

$RMSE_P$ (gm^{-2}) is the root mean square errors in prediction of the simple general model using the independent test data set.

models showed higher R^2 values and predicted AGB with significantly lower $RMSE_P$ values than the simple general models did (Tables 5 and 6). Similar to the simple models, the sophisticated general model between VIUPD and AGB had higher R^2 values and lower prediction errors than the models for NDVI and SAVI. Additionally, there were no apparent differences between prediction errors by models using NDVI and SAVI.

The differences in ecosystem characteristics caused differences in the model structures and parameters. Variations in the selected independent variables for a given VI occurred as the bench ecosystem changed; this led to the differences in the coefficients of determination and the prediction errors. For NDVI, the same model was established by stepwise regression despite switches in the bench ecosystem selection among the degraded meadow, *Achnatherum* grassland, *Stipa* steppe or *Kobresia* meadow. The independent variables of the model were intercept, NDVI and I(degraded steppe). When the degraded steppe was set as the bench ecosystem, the slopes for *Kobresia* meadow and *Achnatherum* grassland were different from the other ecosystems. On the other hand, the selected variables were intercept, NDVI, S(*Kobresia* meadow) and S(*Achnatherum*) when the degraded steppe was chosen as the bench ecosystem. As to SAVI, intercept, SAVI and S(degraded steppe) were selected as predictors when the degraded meadow, *Achnatherum* grassland, *Stipa* steppe or *Kobresia* meadow was set as the bench ecosystem. When the degraded steppe was set as the bench ecosystem, the significant independent variables were intercept, SAVI, S(*Kobresia* meadow), S(*Achnatherum*) and I(degraded meadow). However, the larger number of predictors led to lower prediction accuracy.

The sophisticated general models between AGB and VIUPD had the highest R^2 (0.893 and 0.905) and the lowest $RMSE_P$ (33.18 and 30.15 gm^{-2}) than those for NDVI and SAVI. Setting *Kobresia* meadow as the bench ecosystem led to a higher R^2 and a lower $RMSE_P$ than setting any of the other four sites as the bench ecosystem. When setting the degraded meadow as the bench ecosystem, only S(*Kobresia* meadow) was included in the model. If *Kobresia* meadow was set as the bench ecosystem, S(degraded meadow), S(*Stipa*), S(*Achnatherum*) and S(degraded steppe) were included as predictors in the model. However, this did not result in much improvement in prediction, as indicated by the $RMSE_P$ values.

DISCUSSION

This study aimed to build a general model to estimate AGB from hyperspectral measurements for the five major grassland types on the Tibetan Plateau. Effectiveness of explanatory variables for AGB estimation relies on the radiation absorption in the red band by pigments such as chlorophyll and various types of carotenoid and energy reflection as well as mesophyll multiscattering in the NIR region. However, there were ecosystem type-dependent characteristics that added extra variation to these spectral features. These additional variations in spectral features come from the differences in vegetation type, fractional coverage of vegetation, phenological stage of plant, amount of standing litter and soil type among these ecosystems. First, as shown in Table 1, the dominant species of each ecosystem differed from one another, which could cause differences in canopy structure and result in multiscattering of energy in the NIR band given same AGB value. Second, the vegetation density showed large differences among various ecosystems, as indicated by mean AGB ranging from 65 gm^{-2} for *Stipa* steppe to 232 gm^{-2} for *Kobresia* meadow, leading to great variations in reflectance, particularly in the red band, as indicated in Fig. 2. Third, the large elevation span among

Table 6: Regression models between AGB and each VI including dummy variables

VI	Regression models with dummy variables					
	Bench ecosystem	Selected predictors	Coefficients	*P* value	R^2 R^2(adj)	$RMSE_P$ (gm^{-2})
NDVI	Degraded meadow[a]	Intercept	−91.30	<0.001	0.833	36.97
		NDVI	644.47			
		I(degraded steppe)	−140.00		0.826	
	Degraded steppe	Intercept	-40.55	<0.001	0.805	42.34
		NDVI	384.04			
		S(*Kobresia* meadow)	159.40		0.792	
		S(*Achnatherum*)	157.77			
SAVI	Degraded meadow[b]	Intercept	−102.86	<0.001	0.799	35.75
		SAVI	951.87		0.790	
		S(degraded steppe)	−258.92			
	Degraded steppe	Intercept	−72.27	<0.001	0.809	37.84
		SAVI	635.92			
		S(*Kobresia* meadow)	248.93		0.792	
		S(*Achnatherum*)	204.60			
		I(degraded meadow)	39.96			
VIUPD	Degraded meadow[c]	Intercept	−29.10	<0.001	0.893	33.18
		VIUPD	921.53		0.889	
		S(*Kobresia* meadow)	513.34			
	Kobresia meadow	Intercept	−13.5	<0.001	0.905	30.15
		VIUPD	1357.49			
		S(degraded meadow	−645.75			
		S(*Stipa*)	−653.84		0.895	
		S(*Achnatherum*)	−502.17			
		S(degraded steppe)	−456.61			

For regression with each VI, each of the five ecosystems was set as the bench ecosystem once to test the ecosystem type dependence of dummy variables definition. $RMSE_P$ (gm^{-2}) is the root mean square errors in validation using the independent test data set. I(ecosystem type) and S(ecosystem type) are dummy variables to explain the effects of ecosystem type on the intercept and slope in the function of AGB–VI relationship. R^2 (adj): adjusted R^2. *P* value is the significance level in *F*-test.

[a] There was no difference in the regression model despite changes in the bench ecosystem setting among the four ecosystems: the degraded meadow, *Stipa* steppe, *Kobresia* meadow and *Achnatherum* grassland.

[b] The same as (a), but for SAVI.

[c] There was no difference in the regression model despite changes the bench ecosystem setting among the four ecosystems: the degraded meadow, *Stipa* steppe, the degraded steppe and *Achnatherum* grassland.

grassland types (Table 1) added additional differences in phenological status among these ecosystems; this could cause differences in pigment concentration and thus cause extra variation in reflectance even for similar vegetation density or AGB. There was no apparent difference in AGB level among grassland types (Table 1), but evident difference in the mean reflectance both in red and NIR bands between the degraded steppe and *Kobresia* meadow. Compared with the degraded steppe, the higher reflectance in the red band and lower reflectance in the NIR band of *Kobresia* meadow were mainly caused by differences in phenological status. When the spectra were measured, *Kobresia* meadow was beginning to senesce and the degraded steppe was still growing to seasonal climax. Finally, variations in soil type or standing litter could also result in dramatic changes in reflectance (Numata *et al.* 2008). In this study, there was obvious standing litter within the canopy of *Achnatherum splendens*. The soil water availability and soil type also showed significant variations among the different ecosystems (Table 1). Soil water content is one of the main sources of changes in spectral characteristics of soil (Huete 1988).

Differences in ecosystem characteristics could explain the variations in the performances of each vegetation indices in estimating AGB. Among the seven used narrow-band vegetation indices, RVI, DVI and NDVI are determined from only the red and NIR reflectance bands. Among these three indices, RVI and NDVI are more sensitive to chlorophyll absorption, but can be impacted more easily by variations in soil characteristics and standing litter. Therefore, for densely vegetated *Kobresia* meadow and the degraded steppe, both NDVI and RVI showed

higher R^2 than the other five vegetation indices (Table 4). Furthermore, compared with the degraded steppe, the lower chlorophyll concentration due to senescence of the *Kobresia pygmaea* resulted in the higher coefficients of determination of the regression between AGB and NDVI or RVI. This was caused by the difference in chlorophyll concentration due to different phenological stages of the vegetation in these two ecosystems, as indicated by the reflectance values in the red and NIR regions in Fig. 2. As well known, high chlorophyll concentration directly determines the saturation of red reflectance and in turn the vegetation indices that are calculated from only the red and NIR reflectance. Compared with the degraded steppe with similar vegetation density, the senescing *K.pygmaea* of *Kobresia* meadow had lower chlorophyll concentration and turned to alleviate saturation effect of red reflectance, which resulted in the higher coefficients of determination of regression between AGB and NDVI, RVI or DVI. DVI is sensitive to variations in soil background and standing litter at lower vegetation cover (<20%) and insensitive to variations in vegetation at higher vegetation coverage (>80%). Thus, DVI showed poorer performance than both NDVI and RVI in this study. For *Stipa* steppe and the degraded meadow, the close R^2 values of all the three vegetation indices resulted from lower variation in the soil background and lower vegetation coverage, which could also explain why the three soil-adjusted vegetation indices, SAVI, MSAVI and EVI did not improve estimation of AGB compared with NDVI. SAVI, MSAVI and EVI are considered to eliminate effects of soil background and tend to weaken vegetation signals. Therefore, these indices showed poorer performance than NDVI and RVI for densely vegetated *Kobresia* meadow and the degraded steppe. Close to the area of the triangle defined by the green peak, the chlorophyll absorption minimum and the NIR shoulder in spectral spade, TVI could provide a good estimate at intermediate chlorophyll concentration but poor estimate at both high and low chlorophyll concentration, as indicated in Table 4. VIUPD was reported to be more sensitive than NDVI and EVI at high vegetation density (LAI > 4, Zhang *et al.* 2007). In this study, VIUPD gave the best estimate for the degraded steppe and a good estimate for *Kobresia* meadow, *Achnatherum* grassland and the degraded meadow. And for *Stipa* steppe, the lowest chlorophyll concentration due to senescence was reasonable for the poor performance for VIUPD because VIUPD in this study is based on spectral reflectance of only pure green vegetation and soil while *Stipa purpurea* was beginning to senesce when its spectra was measured. In the Zhang *et al.* (2007) study, VIUPD was calculated from decomposition with four components including water, soil, green vegetation and yellow vegetation and thus showed advantage over NDVI and EVI when coping with samples including senescing leaves. Therefore, yellow vegetation component should be included in case there is senesced leaves in the canopy.

When the regressions were conducted for each ecosystem separately, AGB of each ecosystem was estimated with high accuracy. The sophisticated general models predicted AGB with higher accuracy than the simple pooled ecosystem model since the dummy variables could account for the ecosystem type effects (Table 6). For example, the intercept in the relation between NDVI and AGB for the degraded steppe was different from the intercept for the other four ecosystems if the degraded meadow was set as the bench ecosystem (Table 6). The relationship between NDVI and AGB for the degraded steppe was

$$\mathrm{AGB} = -231.30 + 644.47\mathrm{NDVI}. \quad (9)$$

Thus, an NDVI value <0.359 will result in negative AGB. Therefore, the degraded steppe should be set as the bench ecosystem if AGB was to be estimated from NDVI.

The differences between the R^2 values of the simple general models and the sophisticated general models are the partial R^2, which were 0.125 for NDVI, 0.124 for SAVI and 0.171 for VIUPD. The differences in prediction errors ($RMSE_P$) were 8.35, 15.18 and 19.66 gm^{-2} for NDVI, SAVI and VIUPD, respectively. The larger number of selected dummy variables for VIUPD was reasonable for the more notable improvements by the sophisticated general models compared to the simple models.

CONCLUSIONS

AGB was estimated from narrow-band vegetation indices and VIUPD calculated from *in situ* hyperspectral reflectance for five typical grasslands on the Tibetan Plateau. RVI and NDVI showed strong relationships with AGB for each ecosystem. SAVI and MSAVI were found not suitable for estimating AGB at high chlorophyll concentration but useful in estimating AGB for ecosystems with low and middle vegetation density. VIUPD could predict AGB reliably for both densely and sparsely vegetated areas, but provided poor estimation for *Sitpa* steppe. Though these vegetation indices could predict AGB for each ecosystem separately, their relationships with AGB varied due to the differences in characteristics among the five ecosystems; this resulted in poorer performance of these explanatory variables when AGB was estimated when all ecosystem were pooled. Dummy variables could account for the effects of ecosystem type and significantly improve the predictions of AGB. Regression models between AGB and VIUPD including dummy variables for ecosystem types provided the best prediction among all the candidate predictors, with a $RMSE_P$ of 30.15 gm^2, compared with 159.2 gm^{-2} as the mean of observed AGB in the test data set. These results demonstrate that *in situ* hyperspectral measurements and satellite/airborne remote sensing techniques are a useful tool for estimating AGB of diverse grassland and steppe ecosystems across large spatial scales. Using dummy variables is a practical way to remove variability in AGB estimates due to the presence of multiple ecosystem types.

Satellite/airborne remote sensing techniques are useful for monitoring AGB dynamics because they provide spatial and

historical information on AGB. Although this analysis was based on *in situ* hyperspectral data, the proposed models for AGB estimation could be directly used to estimate AGB from satellite/airborne remotely sensed data when adequate spatial, temporal and spectral resolution data are available from satellite/airborne sensors and when strict atmospheric and topographical corrections are available. While there is considerable heterogeneity in vegetation and soil characteristics across the Tibetan Plateau, the sampling area in this study is small compared with the pixel size of the global operational vegetation indices such as MODIS NDVI, SPOT NDVI and NOAA/AVHRR NDVI. Moreover, the solar and viewing geometry and spectral resolutions of these data also differ from the plot scale, field observation. Therefore, additional research on estimating AGB from remotely sensed images with a high spatial resolution (from dozens of centimeters to several meters) is required to refine our ability to monitor AGB dynamics using these coarse resolution NDVI data.

FUNDING

The field investigation was partly supported by a program on long-term monitoring of alpine ecosystems on the Tibetan Plateau from the Ministry of Environment, Japan to T.Y.; Program for New Century Excellent Talents in University to C.J.; Director-encouragement fund from National Institute for Environmental Studies to S.A.

ACKNOWLEDGEMENTS

We thank the two anonymous reviewers for their valuable comments and suggestions.

REFERENCES

Chapin FS III, Randerson JT, McGuire AD, *et al.* (2008) Changing feedbacks in the climate-biosphere system. *Front Ecol Environ* **6**:313–20.

Curran PJ, Dungan JL, Peterson DL (2001) Estimating the foliar biochemical concentrations of leaves with reflectance spectrometry: testing the Kokaly and Clark Methodologies. *Remote Sens Environ* **76**:349–59.

Elvidge CD, Chen ZK (1995) Comparison of broad band and narrowband and near-infrared vegetation indices. *Remote Sens Environ* **54**:38–48.

Fan J, Zhong H, Harris W, *et al.* (2008) Carbon storage in the grasslands of China based on field measurements of above- and below-ground biomass. *Clim Change* **86**:375–96.

Filella I, Penuelas J, Liorens L, *et al.* (2004) Reflectance assessment of seasonal and annual changes in biomass and CO_2 uptake of a Mediterranean shrubland submitted to experimental warming and drought. *Remote Sens Environ* **90**:308–18.

Friedl MA, Michaelsen J, Davegetation indices FW, *et al.* (1994) Estimating grassland biomass and leaf-area index using ground and satellite data. *Int J Remote Sens* **15**:1401–20.

Hall DO, Rao KK (1987) *Photosynthesis*. Great Britain, Edward Arnold.

Hansen PM, Schjoerring JK (2003) Reflectance measurement of canopy biomass and nitrogen status in wheat crops using normalized difference vegetation indices and partial least square regression. *Remote Sens Environ* **86**:542–33.

Holzgang O (2001) Assessing above-ground phytomass in an alpine region using a hand-held radiometer. *Bot Helv III* 73–85.

Huete AR (1988) A soil-adjusted vegetation index (SAVI). *Remote Sens Environ* **25**:295–309.

Jordan CF (1969) Derivation of leaf area index from quality of light on the forest floor. *Ecology* **50**:663–6.

Kokaly RF, Clark RN (1999) Spectroscopic determination of leaf biochemistry using band depth analysis of absorption features and stepwise multiple linear regression. *Remote Sens Environ* **67**:267–87.

Kumpula T, Colpaert A, Wang Q, *et al.* (2004) Remote sensing in inventory of high altitude pastures of the eastern Tibetan Plateau. *Rangifer* **15**:53–63.

Kutzbach JE, Prell WL, Ruddiman WF (1993) Sensitivity of Eurasian climate to surface uplift of the Tibetan Plateau. *J Geophys Res* **101**:177–99.

Lan Y (2004) The degradation problem and strategy of alpine meadow in Qingzang Plateau. *Qinghai Prataculture* **13**:27–30. (In Chinese with abstract in English).

Liu H, Huete AR (1995) A feedback based modification of the NDVI to minimize canopy background and atmospheric noise. *IEEE Trans Geosci Remote Sens* **33**:457–65.

Luo T, Li W, Zhu H (2002) Estimated biomass and productivity of natural vegetation on the Tibetan Plateau. *Ecol Appl* **12**:980–97.

Manabe S, Terpstra TB (1974) The effects of mountains on the general circulation of the atmosphere as identified by numerical experiments. *J Atmos Sci* **31**:3–42.

Mirik M, Norland JE, Crabtree RL, *et al.* (2005) Hyperspectral one-meter-resolution remote sensing in Yellowstone National Park, Wyoming: II. Biomass. *Rangeland Ecol Manag* **58**:459–65.

Mutanga O, Skidmore AK (2004a) Narrow band vegetation indices overcome the saturation problem in biomass estimation. *Int J Remote Sens* **25**:3999–4014.

Mutanga O, Skidmore AK (2004b) Hyperspectral band depth analysis for a better estimation of grass biomass (*Cenchrus ciliaris*) measured under controlled laboratory conditions. *Int J Appl Earth Obs Geoinformation* **5**:87–96.

Numata I, Roberts DA, Chadwick OA, *et al.* (2008) Evaluation of hyperspectral data for pasture estimate in the Brazilian Amazon using field and imaging spectrometers. *Remote Sens Environ* **112**:1569–83.

Qi J, Chehbouni A, Huete AR, *et al.* (1994) A modified soil adjusted vegetation index. *Remote Sens Environ* **48**:119–26.

Rouse JW, Haas RH, Schell JA, *et al.* (1973) Monitoring vegetation systems in the great plains with ERTS. In: Freden SC, Mercanti EP, Becker MA (eds). *Third previous ERTS Symposium*. Washington, DC: NASA SP-351 I, pp. 309–317.

Rundquist BC (2002) The influence of canopy green vegetation fraction on spectral measurements over native tallgrass prairie. *Remote Sens Environ* **81**:129–35.

Schino G, Borfecchia F, De Cecco L, *et al.* (2003) Satellite estimate of grass biomass in a mountainous range in central Italy. *Agroforestry Syst* **59**:157–62.

Thenkabail PS, Smith RB, De Pauw E (2000) Hyperspectral vegetation indices and their relationships with agricultural crop characteristics. *Remote Sens Environ* **71**:158–82.

Todd SW, Hoffer RM, Milchunas DG (1998) Biomass estimation on grazed and ungrazed rangelands using spectral indices. *Int J Remote Sens* **19**:427–38.

Tucker CJ (1977) Spectral Estimation of Grass Canopy Variables. *Remote Sens Environ* **19**:427–38.

Tucker CJ (1979) Red and photographic infrared linear combinations for monitoring vegetation. *Remote Sens Environ* **8**:127–50.

Zhang LF, Furumi S, Muramatsu K, *et al.* (2007) A new vegetation index based on the universal pattern decomposition method. *Int J Remote Sens* **28**:107–24.